NANO LETTERS

Letter

pubs.acs.org/NanoLett

Conductance of Molecular Junctions Formed with Silver Electrodes

Taekyeong Kim,[†] Héctor Vázquez,[†] Mark S. Hybertsen,*[,‡] and Latha Venkataraman*[,†]

[†]Department of Applied Physics and Applied Mathematics, Columbia University, New York, New York 10027, United States

[‡]Center for Functional Nanomaterials, Brookhaven National Laboratory, Upton, New York 11973, United States

Supporting Information

ABSTRACT: We compare the conductance of a series of amine-terminated oligophenyl and alkane molecular junctions formed with Ag and Au electrodes using the scanning tunneling microscope based break-junction technique. For these molecules that conduct through the highest occupied molecular orbital, junctions formed with Au electrodes are more conductive than those formed with Ag electrodes, consistent with the lower work function for Ag. The measured conductance decays exponentially with molecular backbone length with a decay constant that is essentially the same for Ag and Au electrodes. However, the formation and evolution of molecular junctions upon elongation are very different for these two metals. Specifically, junctions formed with Ag electrodes sustain significantly longer elongation when compared with Au due to a difference in the initial gap opened up when the metal point-contact is broken. Using this observation and density functional theory calculations of junction structure and conductance we explain the trends observed in the single molecule junction conductance. Our work thus opens a new path to the conductance measurements of a single molecule junction in Ag electrodes.

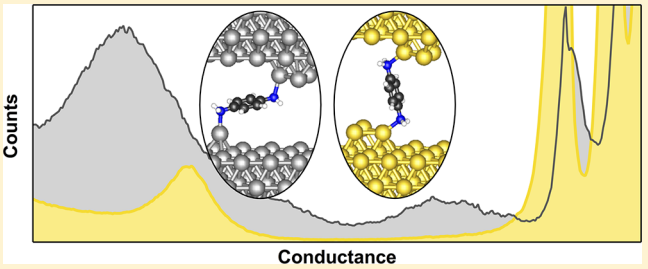

KEYWORDS: *Single-molecule electronics, Ag-molecular junctions, density functional theory, oligophenyls, tunneling decay*

Single molecule−metal junctions form an excellent platform for investigating transport characteristics in nanoscale and organic-based devices. One of the most versatile techniques to create single metal−molecule junctions is using the scanning tunneling microscope based break-junction technique (STM-BJ).[1] Nearly all STM-BJ measurements, however, have been carried out using gold (Au) metal electrodes since Au is chemically inert and hence easy to work with under ambient conditions. Using silver (Ag) as an electrode material could open up interesting avenues due to its strong optical enhancement property[2,3] and its high catalytic activity for certain chemical reactions.[4,5] Furthermore, Ag is similar to Au in terms of atomic and electronic structure, and thus measurements that are possible with Au electrodes should be accessible with Ag electrodes. However the molecular conductance measurements using Ag metal remain challenging to carry out, and little has been done to characterize experimentally and theoretically single molecule junctions with Ag electrodes.[6]

Here, we carry out conductance measurements of a series of amine-terminated oligophenyls and alkanes with both Ag and Au electrodes using the STM-BJ technique. We measure a higher junction conductance with Au electrodes than with Ag. This follows the trend of the work function for the clean surfaces [5.3 eV for Au(111) and 4.7 eV for Ag(111)[7]] for these amine-terminated molecules in which tunneling is primarily mediated by the highest occupied molecular orbital (HOMO). We also see that molecular junction conductance for each series decays exponentially with molecular backbone length for both metals, with tunneling decay constants that are not too different on Ag compared with Au. This is consistent with previous results that find that, in this tunneling transport regime with the electrode Fermi energy relatively far from the HOMO, β is generally independent of electrode work function.[8,9] We do find, however, that the junction formation probability and the evolution of conductance with junction elongation are different for Ag compared with Au. Specifically, with Ag electrodes, we can elongate the molecular junctions to longer distances as compared with Au. We explain this result by comparing the dynamics of the Ag and Au metal point contacts rupture, which precedes the molecular junction formation. Finally, we also find that the Ag-molecule-Ag junction conductance varies more than the Au analog, yielding significantly broader distributions of conductances for statistically significant data sets. We carry out density functional theory (DFT) calculations to understand the origin of these similarities and differences between Ag and Au based single-molecule junctions. Calculations of junction conductance and binding energies for two selected structures and their evolution under elongation show good agreement with the experiment.

We measure the molecular conductance by repeatedly forming and breaking Ag and Au point contacts in the presence of molecules with a modified STM-BJ setup that has been described in detail previously.[10] We use a mechanically polished Ag slug (Alfa-Aesar, 99.99% purity) with a freshly cut Ag wire

Received: May 6, 2013
Revised: May 28, 2013
Published: June 3, 2013

   dx.doi.org/10.1021/nl401654s | *Nano Lett.* 2013, 13, 3358−3364

tip (Alfa-Aesar, 99.9985% purity) for the Ag measurements and an Au/mica substrate with an Au wire tip (Alfa-Aesar, 99.998% purity) for the Au measurements.[11] The STM operates in ambient conditions at room temperature, and the junctions are broken in a 1 mM solution of the molecules in 1,2,4-trichlorobenzene (Sigma-Aldrich, 99% purity). Each conductance measurement starts by moving the tip into the substrate to create a metal point-contact with a conductance of at least $5G_0$.[12] This ensures that a new electrode structure is created for each measurement. The tip is then withdrawn from the substrate at a speed of about 18 nm/s, while the current is recorded at a fixed applied bias voltage of 25 mV at a 40 kHz data acquisition rate. This yields a conductance (current/voltage) versus displacement trace. In all measurements reported here, thousands of curves were collected to allow for a detailed statistical analysis.

Figure 1a shows individual conductance traces from measurements in a solution of 1,4-benzenediamine (**P1**) by

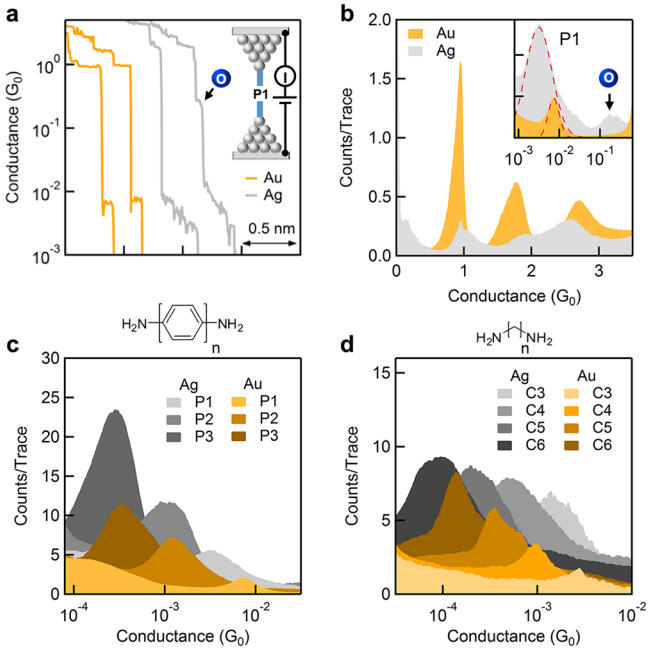

Figure 1. (a) Sample conductance traces for **P1** measured with Au and Ag electrodes. Inset: Illustration of the molecular junction. (b) Normalized one-dimensional conductance histograms for **P1** measurements with Au (28 000 traces) and Ag (7000 traces) generated without data selection using a linear bin size of 0.0001 G_0. Inset: Logarithmically binned conductance histograms generated from the same traces using 100 bins/decade showing the molecular region. The Ag histogram shows an additional peak around 0.2 G_0 possibly due to the formation of an Ag−O−Ag junction. Log-binned conductance histograms for (c) oligophenyls (**P1**−**P3**) and (d) alkanes (**C3**−**C6**) generated using 100 bins/decade.

using Au (yellow) and Ag (gray) metal electrodes, as illustrated in the inset of Figure 1a. These traces highlight the similarities and key differences between Ag and Au measurements. Conductance plateaus at and above 1 G_0 ($G_0 = 2e^2/h$, the quantum of conductance) are formed for both Ag and Au traces. In addition, a clear plateau is seen just below 10^{-2} G_0 in the Au traces due to the formation of stable Au-**P1**-Au junctions.[10] For the Ag traces, we see a sloped plateau starting at a similar conductance, which we attributed to the formation of an Ag-**P1**-Ag junction. We also find that the Ag-**P1**-Ag plateau is significantly longer than that of the Au-**P1**-Au junctions. In addition, some of the traces measured with Ag electrodes have additional features (indicated by the arrow in Figure 1a) between ~0.1 G_0 and 0.7 G_0. These have been attributed to the formation of a junction that includes an oxygen atom in series with the Ag contact (Ag−O−Ag) after the Ag contact is thinned down on elongation.[11,13,14]

Figure 1b shows linear binned conductance histograms measured with **P1** using Ag (gray, 7000 traces) and Au (yellow, 28 000 traces) electrodes without any data selection. Peaks at and above ~1 G_0 are seen in both histograms, although those for Ag are definitely smaller in height than those for Au. This difference in conductance peak heights is due to Ag having shorter 1 G_0 plateaus as seen in the sample traces shown in Figure 1a, as Ag point contacts do not form chains readily.[15−17] The inset of Figure 1b shows histograms created using logarithmic bins to highlight the molecular region. The red dashed curves are the Gaussian fits to the molecular peaks. We can obtain the conductance values from the center of these Gaussian fits using the procedure described by Huber et al.[18] (see Supporting Information). The most probable junction conductance is 6.4×10^{-3} G_0 for Au-**P1**-Au junctions and 2.1×10^{-3} G_0 for Ag-**P1**-Ag junctions. A peak around 0.2 G_0 is also observed in the Ag histogram due to the formation of Ag−O−Ag junctions.[13,14] To check that the molecular conductance peak does not depend on whether individual traces show the Ag−O−Ag feature, we sort through all measured traces and separately create one-dimensional (1D) conductance histograms for traces with and without the oxygen feature (SI, Figure S1). We find no significant difference in the position of the molecular peak in these two histograms and conclude that the oxygen feature does not change the transport characteristics of an Ag-**P1**-Ag junction significantly.

Figures 1c and 1d compare log-binned conductance histograms for measurements with a series of oligophenyls with 1−3 benzene groups (**P1**, **P2**, and **P3**) and alkanes with 3−6 methylene groups (**C3**−**C6**) using Ag and Au electrodes. Each conductance histogram reveals a clear peak at a conductance value that decreases exponentially with molecule length on both electrodes. The width of the conductance histogram peak is consistently wider for Ag measurements when compared with Au. This is most clearly visible for the **C6** data (Figure 1d). To probe the origin of these wide histograms, we create two-dimensional (2D) conductance-displacement histograms from all these data sets. The normalized 2D conductance-displacement histograms for three molecules (**P1**, **P2**, and **C5**) measured with Ag and Au are shown in Figure 2 (and the others are shown in SI, Figure S2). These histograms are created by overlaying all measured conductance traces after aligning them along the displacement axis at a conductance of 0.5 G_0. The data are plotted using logarithmic bins along the conductance axis and linear bins along the displacement axis. We see first that the counts for all measurements with Ag electrodes are significantly higher than those with Au indicating that the probability of junction formation for Ag electrodes is higher for all molecules. For each 2D histogram, we also overlay a conductance profile (black dashed and solid curves), which is determined from the peak locations of the vertical cross sections at all displacement bins.

The 2D histograms show molecular conductance features that are clearly sloped for both **P1** and **P2** on Ag when compared to measurements with Au. In addition, all Ag 2D histograms show a feature just below 1 G_0 that has been

dx.doi.org/10.1021/nl401654s | Nano Lett. 2013, 13, 3358−3364

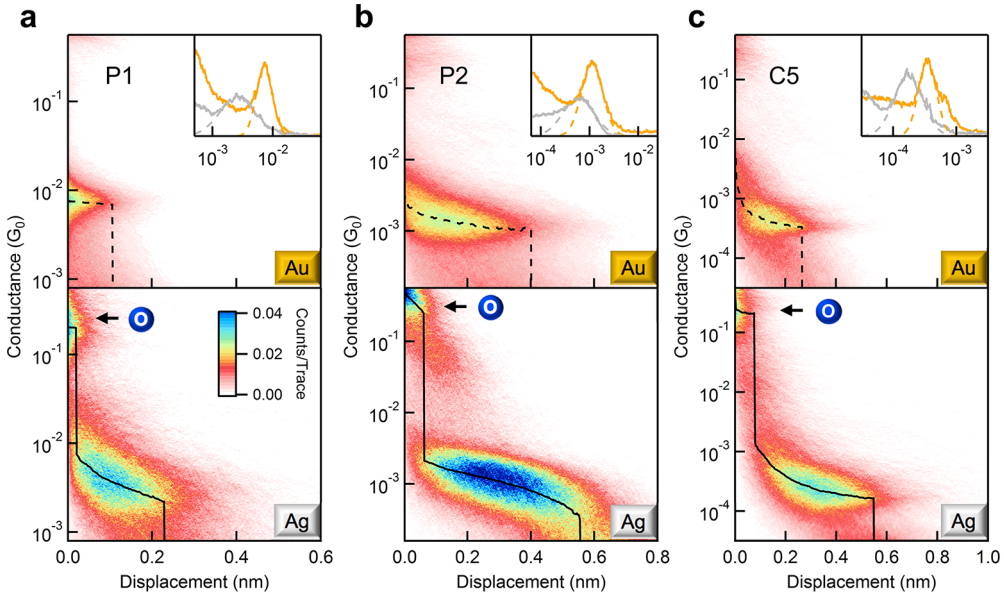

Figure 2. Normalized two-dimensional conductance histograms for **P1** (a), **P2** (b), and **C5** (c) measured with Au (upper panel) and Ag (lower panel) electrodes. Insets in upper panel are conductance profiles (solid curves) and Gaussian fits (dashed curves) determined from 2D histograms over a width of 0.05 nm centered at the end of the molecular feature. The arrow in the lower panel points to the feature due to Ag−O−Ag junctions seen in a large fraction of traces.

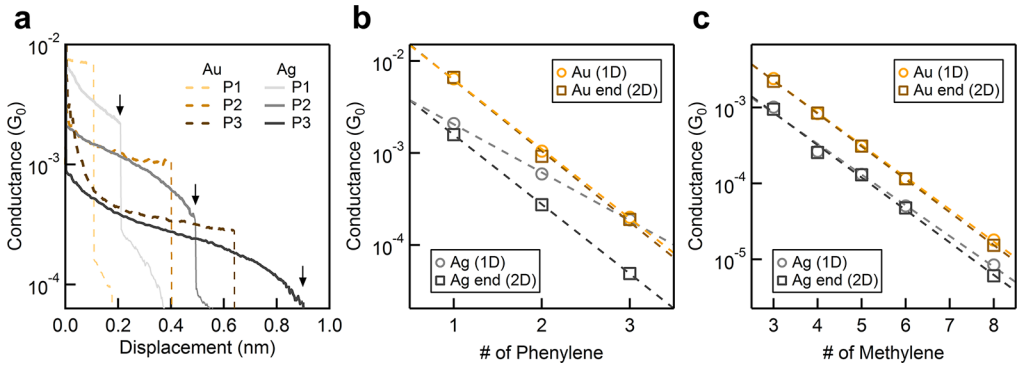

Figure 3. (a) Conductance profiles determined from the 2D histograms for the oligophenyl series measured with both Au electrodes (dashed curves) and Ag electrodes (solid curves). The arrows indicate a fully extended molecular junction just prior to rupture for Ag electrodes. Conductance values determined from 1D histograms (light circles) and from fully elongated junctions (dark squares) for (b) oligophenyls and (c) alkanes, measured with both Au and Ag electrodes. The dashed lines are the linear fits to the data.

attributed to the Ag−O−Ag feature.[11,13,14] The molecular conductance features at any given displacement are wider for Ag measurements when compared with Au measurements. This is highlighted in the inset, which compares profiles taken at the end of the 2D conductance feature for each molecule. The widths of these profiles are compared in SI, Figure S3 for alkanes and oligophenyls. A clear increase in the width is seen for all Ag data when compared with Au data. The increased distribution in conductances measured with Ag electrodes results from a combination of three effects: (a) conductance plateaus are more sloped for Ag measurements, especially for oligophenyls, as evidenced by the 2D histograms, (b) conductance plateaus have more noise as illustrated in sample traces in Figure 1a for **P1** and in SI, Figure S4 for **P2**, and (c) Ag measurements show a larger junction-to-junction variations as seen from sample traces.

Since the junction conductance varies with junction elongation for the Ag measurement, the conductances determined from the histogram peak in Figures 1c and d represent a statistical average over the thousands of junctions measured as well as an average over the length of the conductance plateau. To disentangle the two averages, we focus on the profiles from the 2D histograms. This allows us to determine an average conductance at any given junction elongation length relative to the start of the molecular plateau. Conductance profiles for both Au (dashed curves) and Ag (solid curves) measurements for all oligophenyls are shown in Figure 3a. We have aligned all of these profiles at the start of the molecular conductance feature so as to not include the oxygen junction in this comparison. Analogous data for the alkanes are shown in SI, Figure S5. These profiles show clearly that, when Ag electrodes are used, the junction conductance decreases with elongation for all molecules. In contrast, junctions measured with Au electrodes do not show this dramatic decrease in conductance with junction elongation except at the start of the plateau, possible due to additional through-space conduction.

dx.doi.org/10.1021/nl401654s | *Nano Lett.* 2013, 13, 3358−3364

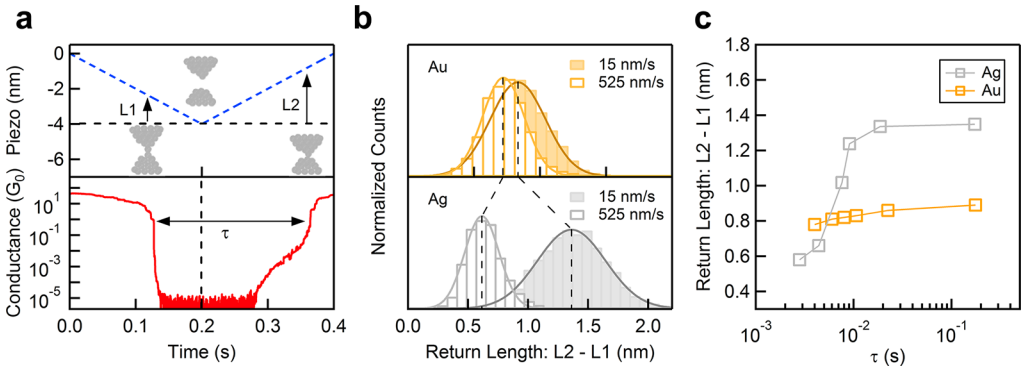

Figure 4. (a) Sample piezo ramp (blue dashed line in the upper panel) and simultaneously acquired conductance trace (red curve in the lower panel) used to measure the gap opened up in a metal point contact after rupture. (b) Histograms of the return length (L2−L1) measured with Au electrodes (upper panel) and Ag electrodes (lower panel) using piezo ramp speeds of 15 and 525 nm/s. Gaussian fits are also shown, and dashed lines indicate the centers. (c) Mean return length plotted against mean τ values (time between contact rupture and reformation) determined for each piezo ramp speed.

We determine the conductance of fully elongated junctions from conductance profiles taken from these 2D histograms as detailed in the SI. We use these conductance values to determine a trend for each molecular backbone type (conjugated oligophenyls and saturated alkanes). We plot, in Figure 3b, the conductance of a fully elongated junction (dark squares) and the conductance obtained from the peaks of the 1D conductance histograms (light circles) for the oligophenyls. For the measurements with Au, the two overlay, in agreement with the observation that the conductance plateaus do not have a significant slope. In contrast, for Ag, there is a clear difference between these two conductance values. The dashed lines are exponential fits to these data (shown on a semilog scale) with $G \propto e^{-\beta N}$ where β is the decay constant and N is the number of units in the chain. We see that the conductance decreases exponentially with an increasing number of phenyls. For Ag, the fits to the 1D histograms and to the elongated junction conductance have different decay constants, while for the Au junctions, both decay constants are similar. As we discuss below, the dependence of the junction conductance on elongation is closely related to different junction structures that can be formed, depending on the gap between the electrodes. If we focus on the end of each of the profiles, then it is most likely that the junction structures will be fully elongated and most comparable. The decay constants determined from the end of the conductance profiles are 1.74 ± 0.05 per phenylene for Ag junctions and 1.78 ± 0.11 per phenylene for Au junctions.

In Figure 3c, we show the analogous data for alkane junctions along with the exponential fits on a semilog scale. For the alkanes, the decay constants do not depend on how the conductance values are determined. The line fits from the conductance of the 1D histogram and the fully elongated junction for both of Ag and Au junctions have almost the same decay constants. This is in agreement with the finding that the alkane plateaus for Ag measurements are not very sloped. The tunneling decay constant, β, determined from these fits is 0.93 ± 0.05 per methylene for the Ag junction and 0.98 ± 0.05 per methylene for the Au junction, respectively. Interestingly, the tunneling decay constants from the conductance of the fully extended junction for oligophenyls and alkanes on both of Au and Ag electrodes are similar. This shows further that for molecules with a large energy gap between the highest occupied molecular orbital (HOMO) and the lowest unoccupied molecular orbital (LUMO), and with the Fermi energy aligned roughly in the middle of the gap, β does not depend significantly on the metal work function. This is consistent with previous findings.[8,9]

We now turn to a second aspect evident in the conductance profiles in Figure 3a: junctions formed with Ag electrodes can be elongated for longer distances than those formed with Au. For example, a **P2** junction can be elongated an additional 1 Å with Ag compared to Au electrodes. Furthermore, the data also show that junctions with **P3** sustain the longest plateaus while those with **P1** sustain the shortest for both metals. To probe the origin of these differences, we first consider the junction formation process. All measurements start with a metal−metal contact that is pulled apart and broken in an environment of molecules. Molecular plateaus are seen after the metal contact ruptures with a plateau length that scales with the molecular backbone length. For Au, this finding has been rationalized by considering the gap that is opened up between the electrodes once the contact ruptures. This has been measured experimentally and found to be about 7 Å.[19,20] Molecules can either insert in this gap, if they are sufficiently short, or they can bind away from the apex atoms on the tip and substrate if they are longer. For the latter case, once a junction is formed, upon elongation, the binding site can move from one atom to the next yielding a conductance plateau that scales with molecular backbone length.[21] The parameter that controls the average conductance plateau length for a given molecule is then the gap formed right after the metal contact ruptures, at the start of the conductance plateau.

To understand the difference in the evolution of Au and Ag junctions, we measure the gap created after Au and Ag metal contacts rupture by following a method detailed before.[20] Briefly, we first form a metal contact, elongate the contact until it ruptures, and then push the electrodes back together to determine the net distance the electrodes need to move before a contact with a conductance of 1 G_0 is formed. This "return length" is measured for both Ag and Au metal contacts without molecules, using different pull/push speeds (v) ranging from 15 to 750 nm/s to also probe the dynamics of the electrode relaxation after the contact ruptures. Figure 4a shows a sample piezo ramp (blue dashed line in the upper panel) and simultaneously acquired conductance trace (red curve in the lower panel). The return length is determined from the difference between the distances L2 and L1 as indicated in the

dx.doi.org/10.1021/nl401654s | Nano Lett. 2013, 13, 3358−3364

figure. Histograms of the return lengths for Au and Ag electrodes measured at two different ramp speeds (15 and 525 nm/s) are shown in Figure 4b (data at all other speeds are shown in SI, Figures S6 and S7). The return lengths for Au (upper panel) decrease slightly as the piezo speed is increased. In contrast, for Ag, we see a significant decrease in the return length as the speed is increased. Specifically, we obtain an average return length of ∼1.3 nm at 15 nm/s, larger than that measured for Au, but only ∼0.6 nm at 525 nm/s, which is smaller than that of Au. For each measured trace, we also determine the time (τ: return length divided by speed) between contact rupture and reformation as shown in Figure 4a. Figure 4c plots the average return length as a function of the average τ determined at each pull speed. We see clearly that, within the accessible time scales in the experiment (about 2−200 ms), the gap opened up in an Ag electrode changes significantly in contrast to results with Au.

We conclude from these measurements that the electrodes undergo an initial relaxation that opens up a small gap of ∼7 Å for Au and ∼5 Å for Ag consistent with previous studies.[19,22,23] This occurs as soon as the contact is ruptured, within the 10 μs time resolution of our experimental setup, and could be due to a relaxation of the electrodes that were elastically stretched in the rupture process. After this fast relaxation, the atoms on the electrodes reorganize to open up a larger gap over a time scale that is dictated by the diffusion constant of the metal. Since Ag has a larger diffusion constant,[24] the electrodes reorganize more quickly, opening up a larger gap within ∼100 ms after rupture. This reorganization time in Au is slower due to its smaller diffusion constant, yielding a relatively time independent return length within the accessible times scales in measurements.

While these dynamics may be further altered in the presence of the molecules with amine end groups that bind to undercoordinated metal sites, the essential point for the present discussion is that the initial gap between electrode tips is smaller by about 1−2 Å in Ag as compared to Au. This qualitatively affects the molecular junction elongations observed in the 2D conductance profiles shown in Figure 3a. At the start of a molecular junction, the gap between the tip and substrate is smaller by about 1−2 Å with Ag when compared with Au. This allows junctions to be extended an additional 1−2 Å before rupture with Ag. With a shorter tip/substrate gap, we can also envisage highly tilted molecular junctions with Ag electrodes that cannot form with Au electrodes.[6]

We carry out density functional theory (DFT) based calculations to probe junction formation energetics, electronic transport characteristics, and evolution of junctions formed with **P1** on both Au and Ag. We pay particular attention to compressed junctions, having a small tip-to-sample distance, motivated by the results of Figure 4c and study the evolution of molecular junctions on both Au and Ag. We carry out DFT-based first-principles calculations of electronic transmission with a gradient-corrected exchange-correlation functional[25] and a nonequilibrium Green's function approach using the SIESTA and TranSIESTA codes.[26,27] Junctions were modeled with a unit cell consisting of six metallic (111) layers, each having 16 atoms, with the molecule bound to either an adatom or a trimer tip structure as shown in Figure 5a. To probe the relation between conductance and electrode separation, we consider junctions where the molecule is in a "vertical" starting position as well as a "horizontal" junction where the molecule is highly tilted in the compressed junction, as shown in the left and right panels in Figure 5a, respectively.

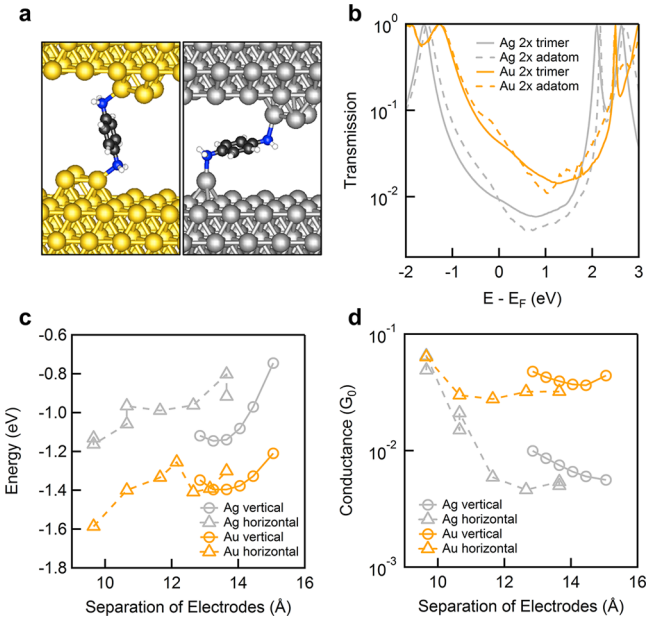

Figure 5. (a) Sample structures showing a vertical (left) and a horizontal (right) junction for **P1** with Au and Ag electrodes, respectively. The upper and lower tip structures for the Ag junction illustrate the trimer and adatom motifs. (b) Transmission curves calculated for the Ag-**P1**-Ag and Au-**P1**-Au junctions using adatom/adatom (dashed curve) and trimer/trimer (solid curve) tips. Binding energy (c), including BSSE corrections, and conductance (d) at E_F for the Ag-**P1**-Ag and Au-**P1**-Au junctions as a function of electrode separation. The triangles indicate horizontal junctions formed using an adatom and a trimer tip. The circles indicate vertical junctions formed using two trimer tips.

In the calculations, we use a single-ζ polarized basis for Au and Ag atoms and a double-ζ polarized basis for molecular atoms. The molecular junction structures are optimized by changing the electrode-electrode separation and minimizing the forces acting on all tip and molecular atoms with a threshold value of 0.02 eV/Å. Binding energies for the junctions are calculated taking into account corrections for basis-set superposition error (BSSE).[28] Transmission calculations are subsequently carried out by adding additional metal electrode layers to the optimized structures. A 5 × 5 Monkhorst-Pack grid and a 250 Ry real-space cutoff are used for the calculation of the electronic structure, while transmission spectra are calculated with a 15 × 15 sampling of the transverse Brillouin zone.

The transmission spectra for **P1** bound in a vertical geometry to Au and Ag are shown in Figure 5b for two tip structures (and analogous transmission curves for **P2** and **P3** are shown in SI, Figure S8). The overall shape of the spectra on Au and Ag are the same, with the spectral features in the case of Ag having a shift of ∼0.2−0.3 eV toward lower energies. This shift is smaller than the difference in work function between Au and Ag (∼0.6 eV for the (111) surfaces) indicating a small difference in the dipole induced by the N−Ag versus the N−Au bond. Although transmission features around the Fermi level are different for adatom−adatom and trimer−trimer junctions, the shape and position of molecular resonances, characterized by peaks in the transmission spectra, are essentially tip-independent. For both Au and Ag, the low-bias transmission of **P1**−**P3** is determined by the HOMO-derived resonance, which falls closest to the Fermi level. The spectra of Au-**P1**-Au for both tip structures

dx.doi.org/10.1021/nl401654s | Nano Lett. 2013, 13, 3358−3364

have a broad HOMO peak and, on the empty part of the spectrum, a rather narrow LUMO-derived resonance, that corresponds to the LUMO having little amplitude on the amine linker groups, and a broader LUMO+1 peak. The case of Ag-**P1**-Ag exhibits, in addition to the downshift of transmission features with respect to Au, narrower molecular resonances, indicative of a weaker electronic coupling. The exception to this is the LUMO, which is broader in Ag due to the larger amplitude of *p*-orbital character near the Fermi energy in Ag. The DFT zero-bias conductance of a **P1** junction with trimer tips is 4.3×10^{-2} G_0 and 9.3×10^{-3} G_0 on Au and Ag, respectively, higher than the measured values due to the well-known overestimation of conductance by DFT-based methods,[29−32] but consistent with earlier work.[30] The calculated conductance of **P1**−**P3** on Au is ∼5 times higher than on Ag, which is consistent with the factor of ∼4 seen in the measured conductance of a fully extended junction. Furthermore, the calculated β values for oligophenyls on Au and Ag electrodes are about 1.6, as shown in SI, Figure S9. These β values are close to those determined from our experimental results.

We now focus on **P1** junctions and study their evolution on Au and Ag electrodes to compare the energetics and conductance of horizontal and vertical structures as a function of junction elongation. Starting from a compressed junction with a small electrode−electrode distance and a highly tilted molecule, the junction structure is optimized, and its conductance is calculated, as described above. The junction is then stretched vertically, increasing the electrode separation, and the process is repeated over a range of ∼4 Å. The binding energies for the junction (for two metal-N bonds) calculated from these trajectories, including BSSE corrections, are shown in Figure 5c. We find that the binding energies for Ag junctions are smaller by about 0.2 eV per bond than those of Au junctions. The geometries from the entire trajectory are energetically accessible in these experiments. For the case of the Ag junctions, we find that junctions can be sustained with the adatom positioned in either of two neighboring surface hollow sites (as shown in SI, Figure S10), resulting in two stable geometries for a given electrode distance as the junction is elongated. In such cases, we consider these two geometries with different locations for the adatom and include data from both in Figure 5c and d. Figure 5d shows the calculated zero bias conductance for all trajectories. We find that the conductance spanned by the Au junctions is significantly narrower than that of the Ag junctions. Furthermore, the conductance of a compressed Ag junction (with the smallest electrode separation) is much higher than that of a fully extended junction. For the case of Au junctions, the entire dynamic range is less than 30% of the mean conductance value, consistent with typical histogram widths observed for **P1**. However, for the Ag electrodes, the range of conductance versus elongation is much bigger (∼120% of the mean conductance value). This traces to the larger sensitivity of electronic coupling to the angle between the Ag tip atom to N bond and N−C bond. Overall, the range of conductance in Figure 5d is consistent with widths of the conductance peaks shown in Figure 1b.

In conclusion we have measured the conductance of molecular junctions formed with amine-terminated oligophenyls and alkanes using both Au and Ag electrodes. Through DFT based calculations, we show that these junctions conduct through the HOMO orbital. We find, in both theory and experiments that Au molecular junctions have a higher conductance than those formed with Ag, consistent with the work function difference for these two metals. Interestingly, we find that junctions formed with Ag can be elongated by longer distances than those formed with Au. We show that this can be explained by examining the dynamics of the metal-contact rupture, where we see that a smaller gap is formed when an Ag-point contact is broken. Our work thus provides an understanding of transport in Ag based molecular junctions through ambient measurements at room temperature.

■ ASSOCIATED CONTENT

Ⓢ Supporting Information

Data analysis and theoretial calculation details; supporting figures. This material is available free of charge via the Internet at http://pubs.acs.org.

■ AUTHOR INFORMATION

Corresponding Author

*E-mail: lv2117@ columbia.edu; mhyberts@bnl.gov.

Present Address

H.V.: Department of Chemistry, University of Warwick, Gibbet Hill Rd CV4 7AL, Coventry, United Kingdom.

Notes

The authors declare no competing financial interest.

■ ACKNOWLEDGMENTS

This work was supported primarily by the NSF under award number DMR-1122594. Part of this work was carried out at the Center for Functional Nanomaterials, Brookhaven National Laboratory, which is supported by the U.S. Department of Energy, Office of Basic Energy Sciences, under contract no. DE-AC02-98CH10886. H.V. was supported through the Nanoscience and Engineering center by the New York State Office of Science, Technology, and Academic Research (NYSTAR). L.V. thanks the Packard Foundation for support.

■ REFERENCES

(1) Xu, B. Q.; Tao, N. J. *Science* **2003**, *301* (5637), 1221−1223.

(2) Jiang, N.; Foley, E. T.; Klingsporn, J. M.; Sonntag, M. D.; Valley, N. A.; Dieringer, J. A.; Seideman, T.; Schatz, G. C.; Hersam, M. C.; Van Duyne, R. P. *Nano Lett.* **2012**, *12* (10), 5061−7.

(3) Lee, S. J.; Baik, J. M.; Moskovits, M. *Nano Lett.* **2008**, *8* (10), 3244−3247.

(4) Lantman, E. M. V.; Deckert-Gaudig, T.; Mank, A. J. G.; Deckert, V.; Weckhuysen, B. M. *Nat. Nanotechnol.* **2012**, *7* (9), 583−586.

(5) Liu, X. Q.; Wang, F.; Niazov-Elkan, A.; Guo, W. W.; Willner, I. *Nano Lett.* **2013**, *13* (1), 309−314.

(6) Kaneko, S.; Nakazumi, T.; Kiguchi, M. *J. Phys. Chem. Lett.* **2010**, *1* (24), 3520−3523.

(7) *CRC Handbook of Chemistry and Physics*, 84th ed.; CRC Press: Boca Raton, FL, 2003−2004.

(8) Engelkes, V. B.; Beebe, J. M.; Frisbie, C. D. *J. Am. Chem. Soc.* **2004**, *126* (43), 14287−14296.

(9) Kim, B.; Choi, S. H.; Zhu, X. Y.; Frisbie, C. D. *J. Am. Chem. Soc.* **2011**, *133* (49), 19864−19877.

(10) Venkataraman, L.; Klare, J. E.; Tam, I. W.; Nuckolls, C.; Hybertsen, M. S.; Steigerwald, M. L. *Nano Lett.* **2006**, *6* (3), 458−462.

(11) Aradhya, S. V.; Frei, M.; Halbritter, A.; Venkataraman, L. *ACS Nano* **2013**, *7* (4), 3706−3712.

(12) Trouwborst, M. L.; Huisman, E. H.; Bakker, F. L.; van der Molen, S. J.; van Wees, B. J. *Phys. Rev. Lett.* **2008**, *100* (17), 175502.

(13) Qi, Y.; Guan, D.; Jiang, Y.; Zheng, Y.; Liu, C. *Phys. Rev. Lett.* **2006**, *97*, 25.

(14) den Boer, D.; Shklyarevskii, O. I.; Coenen, M. J. J.; van der Maas, M.; Peters, T. P. J.; Elemans, J. A. A. W.; Speller, S. *J. Phys. Chem. C* **2011**, *115* (16), 8295−8299.
(15) Smit, R. H. M.; Untiedt, C.; Yanson, A. I.; van Ruitenbeek, J. M. *Phys. Rev. Lett.* **2001**, *87* (26), 266102.
(16) Thijssen, W. H. A.; Marjenburgh, D.; Bremmer, R. H.; van Ruitenbeek, J. M. *Phys. Rev. Lett.* **2006**, *96*, 2.
(17) Thijssen, W. H. A.; Strange, M.; aan de Brugh, J. M. J.; van Ruitenbeek, J. M. *New J. Phys.* **2008**, *10* (3), 033005.
(18) Huber, R.; Gonzalez, M. T.; Wu, S.; Langer, M.; Grunder, S.; Horhoiu, V.; Mayor, M.; Bryce, M. R.; Wang, C. S.; Jitchati, R.; Schonenberger, C.; Calame, M. *J. Am. Chem. Soc.* **2008**, *130* (3), 1080−1084.
(19) Yanson, A. I.; Bollinger, G. R.; van den Brom, H. E.; Agrait, N.; van Ruitenbeek, J. M. *Nature* **1998**, *395* (6704), 783−785.
(20) Quek, S. Y.; Kamenetska, M.; Steigerwald, M. L.; Choi, H. J.; Louie, S. G.; Hybertsen, M. S.; Neaton, J. B.; Venkataraman, L. *Nat. Nanotechnol.* **2009**, *4* (4), 230−234.
(21) Kamenetska, M.; Koentopp, M.; Whalley, A.; Park, Y. S.; Steigerwald, M.; Nuckolls, C.; Hybertsen, M.; Venkataraman, L. *Phys. Rev. Lett.* **2009**, *102* (12), 126803.
(22) Rodrigues, V.; Fuhrer, T.; Ugarte, D. *Phys. Rev. Lett.* **2000**, *85* (19), 4124−4127.
(23) Lagos, M. J.; Autreto, P. A. S.; Galvao, D. S.; Ugarte, D. *J. Appl. Phys.* **2012**, *111* (12), 124316−7.
(24) Ferrando, R.; Tréglia, G. *Surf. Sci.* **1995**, *331*−*333* (Part B, 0), 920−924.
(25) Perdew, J. P.; Burke, K.; Ernzerhof, M. *Phys. Rev. Lett.* **1996**, *77* (18), 3865−3868.
(26) Soler, J. M.; Artacho, E.; Gale, J. D.; Garcia, A.; Junquera, J.; Ordejon, P.; Sanchez-Portal, D. *J. Phys.: Condens. Matter* **2002**, *14* (11), 2745−2779.
(27) Brandbyge, M.; Mozos, J. L.; Ordejon, P.; Taylor, J.; Stokbro, K. *Phys. Rev. B* **2002**, *65* (16), 165401.
(28) van Duijneveldt, F. B.; van Duijneveldt-van de Rijdt, J. G. C. M.; van Lenthe, J. H. *Chem. Rev.* **1994**, *94* (7), 1873−1885.
(29) Koentopp, M.; Burke, K.; Evers, F. *Phys. Rev. B* **2006**, *73* (12), 121403.
(30) Quek, S. Y.; Venkataraman, L.; Choi, H. J.; Louie, S. G.; Hybertsen, M. S.; Neaton, J. B. *Nano Lett.* **2007**, *7* (11), 3477−3482.
(31) Quek, S. Y.; Choi, H. J.; Louie, S. G.; Neaton, J. B. *Nano Lett.* **2009**, *9* (11), 3949−3953.
(32) Strange, M.; Rostgaard, C.; Hakkinen, H.; Thygesen, K. S. *Phys. Rev. B* **2011**, *83* (11), 115108.